Path integrals in fluctuating markets with a non–Gaussian option pricing model

Frédéric D.R. Bonnet[a,b], John van der Hoek[c], Andrew Allison[a,b] and Derek Abbott[a,b]

[a]Department of Electrical and Electronic Engineering, The University of Adelaide, S.A. 5005, Australia.

[b]Centre for Biomedical Engineering, The University of Adelaide, S.A. 5005, Australia.

[c]Department of Applied Mathematics, The University of Adelaide, S.A. 5005, Australia.

ABSTRACT

It is well established that volatility has a memory of the past, moreover it is found that volatility correlations are long ranged. As a consequence the volatility cannot be characterized by a single correlation time. Recent empirical work suggests that the volatility correlation functions of various assets actually decay as a power law. In this paper we show that it is possible to derive the path integral for a non-Gaussian option pricing model that can capture fat–tails. We aim to find the most probable path that contributes to the action functional, that describes the dynamics of the entire system, by finding local minima. We obtain a second order differential equation for the functional return. This paper reviews our current progress and the remaining open questions.

Keywords: Path integrals, fat-tails, non-Gaussian distributions, option pricing, Tsallis distribution.

1. A NON-GAUSSIAN OPTION PRICING MODEL

It is argued that heavy non–Gaussian tails and finite hedging time make it necessary to formulate a model outside the notion of risk–free option prices.[1,2]

As opposed to other models where the standard Black–Scholes price model is extended to account for non normal noise, such as jump diffusion models[3] or Levy noise,[4] here we use a model developed for stock return fluctuations.[5,6] A closed form solution for European options was successfully derived therein. This approach is based on a class of stochastic process that allows statistical feedback as a model of the underlying stock returns. In there it was also shown that the distributions of returns implied by these processes closely matched those found empirically.

In particular, they display features such as fat–tails and peaked middles that are not at all captured by the standard class of log–normal distributions. Such stochastic processes were recently introduced within a Tsallis framework.[7] This framework is used in statistical physics, namely within the field of Tsallis nonextensive thermostatistics.[8,9]

In this setting, we assume that the log return for the stock price $S(t)$ defined as

$$Y(t) \equiv \ln\left[\frac{S(t+\tau)}{S(\tau)}\right], \tag{1}$$

where τ is just an increment constant value. This follows the process

$$dY = \mu\, dt + \sigma\, d\Omega, \tag{2}$$

Further author information: (Send correspondence to Frederic D.R. Bonnet.)
Frederic D.R. Bonnet: E-mail: fbonnet@eleceng.adelaide.edu.au, Telephone: +61 8 8303 6296
John van der Hoek: E-mail: jvanderh@maths.adelaide.edu.au, Telephone: +61 8 8303 5903
Andrew Allison: E-mail: aallison@eleceng.adelaide.edu.au, Telephone: +61 8 8303 5283
Derek Abbott: E-mail: dabbott@eleceng.adelaide.edu.au, Telephone: +61 8 8303 5748

Noise and Fluctuations in Econophysics and Finance, edited by Derek Abbott, Jean-Philippe Bouchaud, Xavier Gabaix, Joseph L. McCauley, Proc. of SPIE Vol. 5848 (SPIE, Bellingham, WA, 2005) · 0277-786X/05/$15 · doi: 10.1117/12.618664

across timescale t, where σ represents the volatility and μ the rate of return. The driving noise is now modeled by Ω, which is drawn from a non–Gaussian distribution.

To do this it is assumed that Ω follows the statistical feedback process,[7]

$$d\Omega = P(\Omega)^{\frac{1-q}{2}}\, dW. \tag{3}$$

These stochastic processes can be interpreted if the driving noise follows a generalized Wiener process governed by a fat–tailed Tsallis distribution[8,9] of index $q > 1$. Hence, using Eq. (3), we may rewrite the stochastic process as

$$dY = \mu\, dt + \sigma\, P(\Omega)^{\frac{1-q}{2}}\, dW. \tag{4}$$

Here W is a Gaussian distributed noise process. For $q = 1$, Ω reduces to W and the standard model is recovered. The probability distribution of the variable Ω evolves according to the non–linear Fokker–Planck equation[7]

$$\frac{\partial}{\partial t}P(\Omega, t|\Omega', t') = \frac{1}{2}\frac{\partial^2}{\partial \Omega^2}P^{2-q}(\Omega, t|\Omega', t'), \tag{5}$$

with P given by the Tsallis distribution and defined as[5–7]

$$P(\Omega, t|\Omega', t') = \frac{1}{Z(t)}\left[1 - \beta(t)(1-q)(\Omega - \Omega')^2\right]^{\frac{1}{1-q}}, \tag{6}$$

In Fig. 1 we show the graphs of Eq. (6) at a fixed q, i.e. at $q = 1.43$, on a fixed interval for $\Omega \in [-1, 1]$. In Fig. 1 (left graph) we can see how the distribution has a slow decaying affect on the tail. These kind of effects are those that are normally observed in real markets. On the opposite side of the scale we may observe that as $t \to 0$ the distribution becomes more and more sharply peaked, see Figure 1 (right graph). This seems to fit quite well the short interval intra–day empirical data from commonly know indexes, like S&P500, Dow Jones and CAC40 for example.

The time dependent $\beta(t)$ function is defined as,

$$\beta(t) = c^{\frac{1-q}{3-q}}\left[(2-q)(3-q)(t-t')\right]^{\frac{-2}{3-q}}, \tag{7}$$

and the normalization factor $Z(t)$ is defined as

$$Z(t) = \left[(2-q)(3-q)c(t-t')\right]^{\frac{1}{3-q}}, \tag{8}$$

and are both plotted in Fig. 2—on the left graph we show $\beta(t)$ as a function of the parameter $1.3 \leq q \leq 2.5$ and the time evolution parameter t and on the right graph $Z(t)$ also as a function of the parameter $1 < q \leq 2.5$ and the time evolution parameter t. In these graphs we can see that in range of $1 < q \leq 2$ the function is well behaved and that there are no singularities. The singularities arise from the Gamma function in the c coefficient, given in Eq. (10).

The q–dependent constant c is given by

$$c = \beta(t)Z^2(t), \tag{9}$$

and is found to be given by the following

$$c \equiv \frac{\pi}{q-1}\frac{\Gamma^2\left(\frac{1}{q-1} - \frac{1}{2}\right)}{\Gamma^2\left(\frac{1}{q-1}\right)}, \tag{10}$$

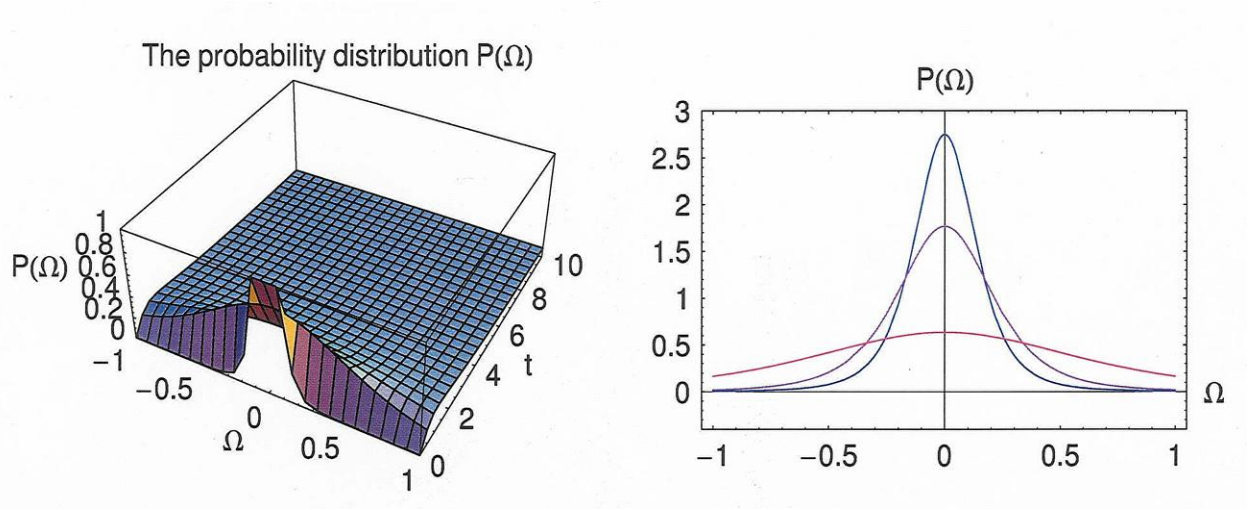

Figure 1. The graph of the probability distribution function Eq. (6) when $q = 1.43$ for the time range of $t \in [0.01, 10]$ and $-1 \leq \Omega \leq 1$ (right graph). We can see that as $t \to 0$ the distribution becomes sharply peaked which diverges to infinity. A two dimensional representation of Fig. 1 for the probability distribution function $P(\Omega)$ versus Ω for $\Omega \in [-1, 1]$, Eq. (6), when $q = 1.43$ at fixed time values. The most sharply peaked curve is when $t = 0.01$, the one in the middle is at $t = 0.05$ and the flattest one is when $t = 0.1$.

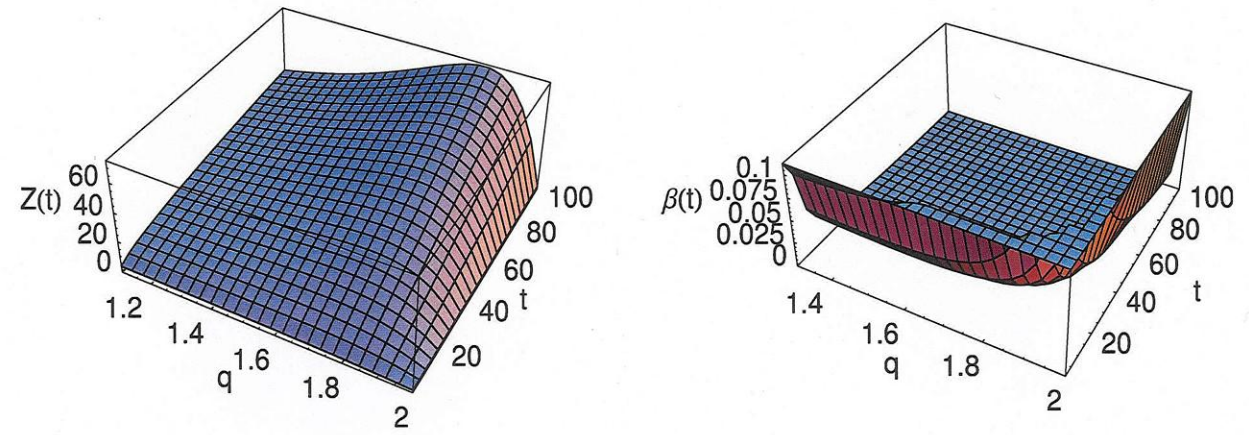

Figure 2. The graph of $\beta(t)$ (left graph) as a function of the parameter $1.3 \leq q \leq 2.5$ and the time evolution parameter t. The graph of $Z(t)$ (right graph) as a function of the parameter $1 < q \leq 2.5$ and the time evolution parameter t.

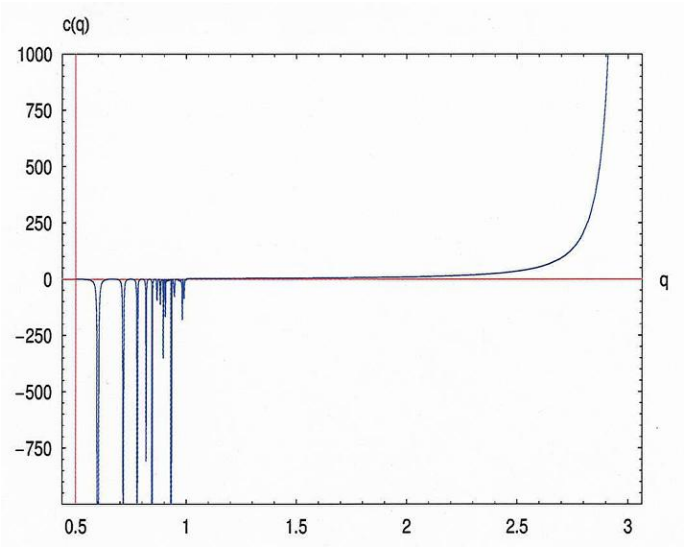

Figure 3. The evolution of the the coefficient c as a function of the parameter q. We can see that in the region $1 < q \leq 3$ the function is well behaved.

where Γ is the usual gamma function. In Fig. (3) we can see that for $q < 1$ the gamma function makes the c function highly divergent. The coefficient c is well behaved from in the range of $1 < c \leq 2.5$. For $q \geq 2.5$ the function diverges to a sharp peak.

We therefore have a non-Gaussian stochastic model that takes the form of

$$dY = \mu\, dt + \frac{\sigma}{[(2-q)c(3-q)\, t]^{\frac{1-q}{2(3-q)}}} \left[1 - c^{\frac{1-q}{3-q}} \left[(2-q)(3-q)t\right]^{\frac{-2}{3-q}} (1-q)\Omega\right]^{\frac{1}{2}} dW, \tag{11}$$

which clearly reduces to Eq. (2) for $q = 1$.

This is the model that we will insert into the path integral to extract the transition probabilities so that we can calculate the option price.

The outline of the paper is as follows. Section 2.1.1 reviews the concept of path integral for the Black–Scholes,[10] Section 3 shows how the path integral is obtained for the non–Gaussian model described in Section 1. Section 4 describes the instanton method. The instanton method is useful in complicated systems because it uses the principle of least action to determine the most probable path contribution to the action functional. The instanton path, in physics gives a prescription in the way one can tunnel from one quantum state to the other. Finally a quick summary of the paper is given in Section 5

2. REVIEWING THE PATH INTEGRAL APPROACH

2.1. The path integral in financial modeling

In the following section we formulate the method such that it becomes more transparent as well as being more applicable in the context of finance. We follow the terminology used by Linetsky.[10]

2.1.1. The path integral for the Black–Scholes model

We start this review section with the formulation of the path integral for the standard Black–Scholes[11] and Merton[12] approach; see also Hull.[4] In this section we will be adopting the Linetsky[10] notation.

A path–independent option is defined by its payoff at expiration time T,

$$\mathcal{O}_{\mathcal{F}}(S_T, T) = \mathcal{F}(S_T), \tag{12}$$

where $\mathcal{F}$ is a given function of the terminal asset price S_T. In the Black–Scholes setting, the risk free interest rate r is continuously compounded and the single risky asset price follows a standard geometric Brownian motion,

$$\frac{dS}{S} = m\,dt + \sigma\,dz, \tag{13}$$

with constant drift rate m and volatility σ. Then the standard absence of no–arbitrage argument leads us to the Black–Scholes partial differential equation (PDE) for the present value of the option at time t preceeding expiration,

$$\frac{\sigma^2}{2}S^2\frac{\partial^2\mathcal{O}_{\mathcal{F}}}{\partial S^2} + rS\frac{\mathcal{O}_{\mathcal{F}}}{\partial S} - r\mathcal{O}_{\mathcal{F}} = -\frac{\mathcal{O}_{\mathcal{F}}}{\partial t}, \tag{14}$$

with initial condition as in Eq. (12). This is also commonly known as the backward Kolmogorov equation for the risk neutral diffusion process, Eq. (13), with drift rate equal to the risk free rate r. Introducing a new variable $x = \ln S$, which follows standard Brownian motion, we find using the general form of Ito lemma,

$$\begin{aligned} d\ln S &= \frac{1}{S}mS\,dt + \sigma S\frac{1}{S}\,dz - \frac{1}{2S^2}\sigma^2S^2\,dt \\ dx &= \left(m - \frac{\sigma^2}{2}\right)dt + \sigma\,dz. \end{aligned} \tag{15}$$

Equation (14) may then be written as

$$\frac{\sigma^2}{2}\frac{\partial^2\mathcal{O}_{\mathcal{F}}}{\partial x^2} + \mu\frac{\mathcal{O}_{\mathcal{F}}}{\partial x} - r\mathcal{O}_{\mathcal{F}} = -\frac{\mathcal{O}_{\mathcal{F}}}{\partial t}, \quad \text{with } \mu = r - \frac{\sigma^2}{2}, \tag{16}$$

and the payoff as $\mathcal{O}_{\mathcal{F}}(e^{x_T}, T) = \mathcal{F}(e^{x_T})$. Eq. (16) is a Cauchy problem, with a solution given by the Feynman–Kac formula

$$\mathcal{O}_{\mathcal{F}}(S,t) = e^{-r\tau}E_{(t,S)}\left[\mathcal{F}(S_T)\right] \quad , \quad \tau = T - t, \tag{17}$$

where $E_{(t,S)}\left[\mathcal{F}(S_T)\right]$ denotes averaging over the risk neutral measure conditional on the initial price S at time t. This average can be represented as an integral over the set of all paths originating from (t, S), called the path integral.

This is defined as a limit of the sequence of finite dimensional multiple integrals, in much the same way as the standard Riemann integral, which is defined as a limit of the sequence of finite sums.[13]

So in the Feynman notation, Eq. (17) is represented as follows with $x = \ln S$ and $x_T = \ln S_T$,

$$\mathcal{O}_{\mathcal{F}}(S,t) = e^{-r\tau}E_{(t,S)}\left[\mathcal{F}(e^{x_T})\right] = e^{-r\tau}\int_{-\infty}^{\infty}\left(\int_{x(t)=x_t}^{x(T)=x_T}\mathcal{F}(e^{x_T})e^{-A_{\mathrm{BS}}\left[x(t')\right]}\mathcal{D}x(t')\right)dx_T. \tag{18}$$

Here $\mathcal{D}$ should be interpreted as a short hand notation for the integration measure for the path integral. The main aspect of this formula is the appearance of the action functional $A_{\mathrm{BS}}\left[x(t')\right]$ defined on the path $\{x(t'), t \le t' \le T\}$ as a time integral of the Black–Scholes Lagrangian function:

$$A_{\mathrm{BS}}\left[x(t')\right] = \int_t^T \mathcal{L}_{\mathrm{BS}}\,dt', \qquad \text{where} \qquad \mathcal{L}_{\mathrm{BS}} = \frac{1}{2\sigma^2}\left(\dot{x}(t') - \mu\right)^2, \quad \text{and} \quad \dot{x}(t') \equiv \frac{dx}{dt'}. \tag{19}$$

This action functional defines then, the path integration measure. The path integral in Eq. (18) is defined as follows. First, the paths are discretized. Time to expiration τ is discretized into N equal time steps Δt bounded by $N-1$ equally spaced time points $t_i = t + i\Delta t$ for each $i = 0, 1, ..., N$ and the time increment is defined as $\Delta t = (T-t)/N$. Discrete prices at these time points are denoted by $S_i = S(t_i)$.

The discretized action functional becomes a function of $N+1$ variables x_i,

$$A_{\mathrm{BS}}(x_i) = \frac{\mu^2\tau}{2\sigma^2} - \frac{\mu}{\sigma^2}(x_T - x) + \frac{1}{2\sigma^2\Delta t}\sum_{i=0}^{N-1}(x_{i+1} - x_i)^2 . \tag{20}$$

This is obtained directly from the definition in Eq. (19)

$$\begin{aligned} \mathcal{L}_{\mathrm{BS}} = \frac{1}{2\sigma^2}\left(\dot{x}(t') - \mu\right)^2 &= \frac{1}{2\sigma^2}\left(\dot{x}^2(t') - 2\dot{x}(t')\mu + \mu^2\right), & (21)\\ A_{\mathrm{BS}}\left[x(t')\right] = \int_t^T \mathcal{L}_{\mathrm{BS}}\, dt' &= \int_t^T \frac{1}{2\sigma^2}\left(\dot{x}^2(t') - 2\dot{x}(t')\mu + \mu^2\right) dt' \\ &= \frac{\mu^2\tau}{2\sigma^2} - \frac{\mu}{\sigma^2}(x_T - x) + \frac{1}{2\sigma^2}\int_t^T \dot{x}^2(t')\, dt'. & (22) \end{aligned}$$

If we set $\mathcal{L}_0 = \frac{1}{2\sigma^2}\int_t^T \dot{x}^2(t')\, dt'$ we see that $\mathcal{L}_0$ represents the Lagrangian for a zero drift process $dx = \sigma\, dz$.

The integrals are discretized by discrete sums such that

$$\int_t^T \cdots dt' \longrightarrow \sum_{i=0}^{N-1} \cdots \Delta t, \tag{23}$$

the derivative term $\dot{x}(t')$ is itself discretized by

$$\dot{x}(t') \longrightarrow \frac{x_{i+1}(t') - x_i(t')}{\Delta t}. \tag{24}$$

Now the path integral over all paths from the initial state $x(t)$ to the final state x_T is defined as

$$\begin{aligned} \int_{x(t)=x_t}^{x(T)=x_T} \mathcal{F}(e^{x_T}) e^{-A_{\mathrm{BS}}\left[x(t')\right]} \mathcal{D}x(t') &\equiv \lim_{N\longrightarrow\infty} \int_{-\infty}^{\infty}\cdots\int_{-\infty}^{\infty} \mathcal{F}(e^{x_T}) e^{-A_{\mathrm{BS}}(x_i)} \frac{dx_1}{\sqrt{2\pi\sigma^2\Delta t}} \cdots \frac{dx_{N-1}}{\sqrt{2\pi\sigma^2\Delta t}} & (25)\\ &\equiv \lim_{N\longrightarrow\infty} \frac{1}{(\sqrt{2\pi\sigma^2\Delta t})^{N-1}} \int_{-\infty}^{\infty}\cdots\int_{-\infty}^{\infty} \mathcal{F}(e^{x_T}) e^{-A_{\mathrm{BS}}(x_i)} dx_1 \cdots dx_{N-1}. \end{aligned}$$

This definition is used in quantum physics.[14] Since we are working with path independent options, the payoff function $\mathcal{F}$ in Eq. (18) can be moved outside of the path integral and can be written as

$$\mathcal{O}_{\mathcal{F}}(S,t) = e^{-r\tau} E_{(t,S)}\left[\mathcal{F}(e^{x_T})\right] = e^{-r\tau}\int_{-\infty}^{\infty} \mathcal{F}(e^{x_T}) \exp\left[\frac{\mu}{\sigma^2}(x_T - x) - \left(\frac{\mu^2\tau}{2\sigma^2}\right)\right] \mathcal{K}(x_T, T|x, t)\, dx_T, \tag{26}$$

where $\mathcal{K}(x_T, T|x, t)$ is the transition probability density for the zero drift Brownian motion $dx = \sigma\, dz$, or commonly known as the propagator in quantum physics,

$$\begin{aligned} \mathcal{K}(x_T, T|x, t) &= \int_{x(t)=x_t}^{x(T)=x_T} e^{-A_0\left[x(t')\right]} \mathcal{D}x(t') & (27)\\ &= \lim_{N\longrightarrow\infty} \frac{1}{(\sqrt{2\pi\sigma^2\Delta t})^{N-1}} \int_{-\infty}^{\infty}\cdots\int_{-\infty}^{\infty} \exp\left[\frac{1}{2\sigma^2\Delta t}\sum_{i=0}^{N-1}(x_{i+1} - x_i)^2\right] dx_1 \cdots dx_{N-1}. \end{aligned}$$

The multiple integral here is then a Gaussian, and it is then possible to use the following integral identity

$$\int_{-\infty}^{\infty} \exp\left[-a(x-z)^2 - b(z-y)^2\right]\, dz = \sqrt{\frac{\pi}{a+b}} \exp\left[-\frac{ab}{a+b}(x-y)^2\right]. \tag{28}$$

Applying this identity to the first integral to with respect to x_1 we see that it reduces to

$$\begin{aligned} \frac{1}{2\pi\sigma^2\Delta t}\int_{-\infty}^{\infty} \exp\left[-\frac{1}{2\sigma^2\Delta t}\left((x_2-x_1)^2+(x_1-x_0)^2\right)\right]\, dx_1 &= \frac{1}{2\pi\sigma^2\Delta t}\sqrt{\frac{\pi}{\frac{1}{2\sigma^2\Delta t}+\frac{1}{2\sigma^2\Delta t}}} \\ &\times \exp\left[-\frac{1}{2\sigma^2 2\Delta t}(x_2-x_0)^2\right] \\ &= \frac{1}{\sqrt{2\pi\sigma^2(2\Delta t)}} \exp\left[-\frac{1}{2\sigma^2(2\Delta t)}(x_2-x_0)^2\right]. \end{aligned} \tag{29}$$

Examining Eq. (29), we observe that the effect of performing one integration introduces a multiplication factor Δt in both the square root and in the exponential terms to replace $(x_2 - x_1) - (x_1 - x_0)$ with $(x_2 - x_0)$. Performing $N-1$ integrals would lead us to multiply the Δt term N times, which we will call $\tau = N\Delta t$. We also observe that the term $(x_T - x)^2$ takes place in the exponential instead of the indexed x. Hence we obtain using Eq. (28) a simple expression for the propagator of the form

$$\mathcal{K}(x_T, T|x, t) = \frac{1}{\sqrt{2\pi\sigma^2\tau}} \exp\left[-\frac{1}{2\sigma^2\tau}(x_T - x)^2\right], \tag{30}$$

which is the normal density. This density function is the fundamental solution of the zero drift diffusion equation

$$\frac{\sigma^2}{2}\frac{\partial^2\mathcal{K}}{\partial x^2} = -\frac{\partial\mathcal{K}}{\partial t}, \tag{31}$$

with the Dirac delta function situated at time $t = T$ as the initial condition,

$$\mathcal{K}(x_T, T|x, t) = \delta(x_T - x). \tag{32}$$

With such settings it can be shown[10] that the diffusion equation can be solved directly, with and without a drift rate μ. In case of the presence of a non–zero constant drift rate μ, as in the Black–Scholes equation, the propagator then becomes

$$\begin{aligned} \mathcal{K}_\mu(x_T, T|x, t) &= \exp\left[\frac{\mu}{\sigma^2}(x_T - x) - \left(\frac{\mu^2\tau}{2\sigma^2}\right)\right]\mathcal{K}(x_T, T|x, t) \\ &= \frac{1}{\sqrt{2\pi\sigma^2\tau}} \exp\left[-\frac{1}{2\sigma^2\tau}\left(-2\tau\mu(x_T - x) + \mu^2\tau^2 + (x_T - x)^2\right)\right] \\ &= \frac{1}{\sqrt{2\pi\sigma^2\tau}} \exp\left[-\frac{1}{2\sigma^2\tau}(x_T - x - \mu\tau)^2\right], \end{aligned} \tag{33}$$

which satisfies the fundamental solution of the diffusion equation with drift

$$\frac{\sigma^2}{2}\frac{\partial^2\mathcal{K}_\mu}{\partial x^2} + \mu\frac{\partial\mathcal{K}_\mu}{\partial x} = -\frac{\partial\mathcal{K}_\mu}{\partial t}. \tag{34}$$

It may also be shown that the transition probability satisfies the fundamental Chapman–Kolmogorov semigroup property (with continuous–time Markov property),

$$\mathcal{K}(x_3, t_3|x_1, t_1) = \int_{-\infty}^{\infty} \mathcal{K}(x_3, t_3|x_2, t_2)\mathcal{K}(x_2, t_2|x_1, t_1)\, dx_2. \tag{35}$$

Consequently, we see how to obtain a definition of the path integral via a repeated use of the Chapman–Kolmogorov equation, hence the path integral written in Eq. (30) may be rewritten as

$$\mathcal{K}(x_T,T|x,t)=\lim_{N\longrightarrow\infty}\int_{-\infty}^{\infty}\cdots\int_{-\infty}^{\infty}\mathcal{K}(x_T,T|x_{N-1},t_{N-1})\cdots\mathcal{K}(x_1,T_1|x,t)\,dx_1\cdots dx_{N-1}. \tag{36}$$

Substituting $\mathcal{K}(x_T,T|x,t)$ into Eq. (26) one obtains the Black–Scholes formula for a path independent option,

$$\begin{aligned}\mathcal{O}_{\mathcal{F}}(S,t) &= e^{-r\tau}\int_{-\infty}^{\infty}\mathcal{F}(e^{x_T})\mathcal{K}_{\mu}(x_T,T|x,t)\,dx_t\\ &= e^{-r\tau}\int_{-\infty}^{\infty}\mathcal{F}(e^{x_T})\frac{1}{\sqrt{2\pi\sigma^2\tau}}\exp\left[-\frac{1}{2\sigma^2\tau}\left(x_T-x-\mu\tau\right)^2\right]dx_T.\end{aligned} \tag{37}$$

For a call option with payoff $\max(e^{x_T}-K,0)$ after performing the integration, one obtains

$$C(S,t)=SN(d_2)-e^{-r\tau}KN(d_1),\quad\text{with} \tag{38}$$

$$d_1=\frac{\ln\left(\frac{S}{K}\right)+\mu\tau}{\sigma\sqrt{\tau}},\quad\text{and}\quad d_2=d_1+\sigma\sqrt{\tau}. \tag{39}$$

It is important to note that in this simple case one does not need such complicated machinery, like path integrals, in order to obtain the transition probabilities in a closed form. However the method of path integrals becomes a lot more useful when one is dealing with a more complicated model as we will see in the subsequent sections.

3. THE PATH INTEGRAL FOR EUROPEAN CALL OPTION WITH A NON–GAUSSIAN OPTION PRICING MODEL

We now explore a model that captures effects, such as fat-tails, that are commonly observed in real markets. It is a well establish fact that models describing the dynamics of real markets have a non-Gaussian nature.

In general, options are usually products issued by financial institutions that give the right but not the obligation to buy (call option) or sell (put option) an asset at a given maximum price (strike price) at a certain given date in the future (expiration date).

In the pool of option strategies, one of the simplest type of options are called European options. A European call option is such that the option holder has the right but not the obligation to buy the underlying asset S at the strike price K on the day of expiration T. Depending of the value of $S(T)$, the payoff of such option is

$$\mathcal{O}=\max\left[S(T)-K,0\right]. \tag{40}$$

In other words if $S(T)>K$ then the terminal asset price S_T will have a value. A path–independent option is defined by its payoff at expiration time T

$$\mathcal{O}_{\mathcal{F}}(S_T,T)=\mathcal{F}(S_T), \tag{41}$$

where $\mathcal{F}$ is a given function of the terminal asset price S_T. Here we are going to be working with the return Ω and not the asset price S directly. The two are related via the ratio of the log of the asset at a given time t. A unique solution to the Cauchy problem is given by the Feynman–Kac formula

$$\mathcal{O}_{\mathcal{F}}(\Omega,t)=e^{-r\tau}E_{(t,\Omega)}\left[\mathcal{F}(\Omega_T)\right],\quad\tau=T-t, \tag{42}$$

where $E_{(t,\Omega)}\left[\mathcal{F}(\Omega_T)\right]$ denotes averaging over the risk neutral measure conditional on the initial stock price S at time t. Here the payoff is defined as

$$\mathcal{F}(\Omega_T)=\frac{1}{Z(T)}S_0\exp\left[\sigma\Omega_T+rT-\sigma^2\alpha T^{\frac{2}{3-q}}\left[1-\beta(T)(1-q)\Omega_T^2\right]\right]\left(1-\beta(T)(1-q)\Omega_T^2\right)^{\frac{1}{1-q}}. \tag{43}$$

This average payoff can be represented as an integral over the set of all paths originating from (t, Ω), called the path integral.

This is defined as a limit of the sequence of finite dimensional multiple integrals, in a much the same way as the standard Riemann integral, which is defined as a limit of the sequence of finite sums.[13]

So in the Feynman notation, Eq. (42) is represented as follows,

$$\mathcal{O}_{\mathcal{F}}(\Omega, t) = e^{-r\tau} E_{(t,\Omega)} \left[\mathcal{F}(\Omega_T)\right] = e^{-r\tau} \int_{-\infty}^{\infty} \left(\int_{\Omega_0}^{\Omega_T} \mathcal{F}(\Omega_T) e^{-A\left[\Omega(t')\right]} \mathcal{D}\Omega(t') \right) d\Omega_T. \tag{44}$$

The main aspect in this formula is the appearance of the action functional $A\left[\Omega(t')\right]$ defined on the path $\{\Omega(t'), t \leq t' \leq T\}$ as a time integral of the Lagrangian function:

$$A\left[\Omega(t')\right] = \int_t^T \mathcal{L}\, dt', \qquad \text{where} \qquad \mathcal{L}(\Omega, \dot{\Omega}) = \frac{1}{2P[\Omega(t')]^{(1-q)}} \left(\dot{\Omega}(t')\right)^2, \quad \text{and} \quad \dot{\Omega}(t') \equiv \frac{d\Omega}{dt'}. \tag{45}$$

This represents the Lagrangian for a zero drift process.

The integral and the derivative terms are discretized as follows: first, the paths are discretized. Time to expiration τ is discretized into N equal time steps Δt bounded by $N-1$ equally spaced time points $t_i = t + i\Delta t$ for each $i = 0, 1, ..., N$ and the time increment is defined as $\Delta t = (T - t)/N$. Discrete prices at these time points are denoted by $\Omega_i = \Omega(t_i)$.

The integrals are discretized by discrete sums such that

$$\int_t^T \cdots dt' \longrightarrow \sum_{i=0}^{N-1} \cdots \Delta t, \tag{46}$$

and the derivative term $\dot{\Omega}(t')$ is itself discretized by

$$\dot{\Omega}(t') \longrightarrow \frac{\Omega_{i+1} - \Omega_i}{\Delta t} \quad \text{with} \quad \Omega_i \equiv \Omega(t_i'). \tag{47}$$

As a result we can rewrite the action functional in its discrete form as

$$\begin{aligned} A\left[\Omega_i\right] &= \sum_{i=0}^{N-1} \mathcal{L}(\Omega_i, \dot{\Omega}_i)\, \Delta t \\ &= \sum_{i=0}^{N-1} \frac{1}{2P(\Omega_i)^{(1-q)}} \dot{\Omega}_i^2\, \Delta t. \end{aligned} \tag{48}$$

Now inserting this action functional into the path integral, Eq. (44), along with Eqs.(6) and (43) we get the following equation for the path integral,

$$\begin{aligned} \mathcal{O}_{\mathcal{F}}(\Omega, t) &= e^{-r\tau} E_{(t,\Omega)} \left[\mathcal{F}(\Omega_T)\right] = e^{-r\tau} \int_{-\infty}^{\infty} \left(\int_{\Omega_0}^{\Omega_T} \mathcal{F}(\Omega_T) e^{-A\left[\Omega(t')\right]} \mathcal{D}\Omega(t') \right) d\Omega_T. \\ &= e^{-r\tau} \int_{-\infty}^{\infty} \left(\lim_{N \longrightarrow \infty} \int_{-\infty}^{\infty} \cdots \int_{-\infty}^{\infty} \mathcal{F}(\Omega_T) e^{-A[\Omega_i]} \prod_{i=1}^{N-1} \frac{d\Omega_i}{\sqrt{2\pi P \left[\Omega_i\right]^{(1-q)} \Delta t}} \right) d\Omega_T. \end{aligned} \tag{49}$$

Now concentrating on the path integral and inserting Eq. (43) and Eq. (48), we obtain

$$\mathcal{O}_{\mathcal{F}}(\Omega, t) = e^{-r\tau} \int_{-\infty}^{\infty} \left(\lim_{N \longrightarrow \infty} \int_{-\infty}^{\infty} \cdots \int_{-\infty}^{\infty} \frac{1}{Z(t)} \left[S_0 \exp\left[\sigma\Omega_T + rT - \sigma^2 \alpha T^{\frac{2}{3-q}} \left[1 - \beta(T)(1-q)\Omega_T^2\right] \right] \right] \right.$$

$$\times \left(1-\beta(T)(1-q)\Omega_T^2\right)^{\frac{1}{1-q}} \exp\left[-\sum_{i=0}^{N-1}\frac{1}{2P[\Omega_i]^{(1-q)}}\dot{\Omega}_i^2\,\Delta t_i\right]\prod_{i=1}^{N-1}\frac{d\Omega_i}{\sqrt{2\pi P\,[\Omega_i]^{(1-q)}\,\Delta t}}\Bigg)\,d\Omega_T. \tag{50}$$

Eq. (50) is the path integral representation for the option price for a European option with the payoff functional described by Eq. (43). There are several ways in evaluating Eq. (50), one of them is to go and directly evaluate the $N-1$ integrals, either by pairing them or one at the time, in that case one either makes some assumption about Ω_i or just directly integrates with respect to Ω_i. Another method is actually get some insight on the analytical form of Ω_i, use this information to insert into the path integral. One way of doing that, is to find the path that contributes the most to the path integral by find an expression for Ω_i that minimizes the action. This is known as the instanton method.

4. THE INSTANTON METHOD

The instanton method is useful in complicated systems because it uses the principle of least action to determine the most probable path contribution to the action functional.

The fundamental quantity of classical mechanics is the action, which is the time integral of the Lagrangian as defined in Eq. (19). The action functional has the ability to describe the entire dynamics of the system over the space in question. In other words this functional contains all of the information about the dynamics of the system.

The principle of least action states that when a system evolves from one given configuration to another between times t_1 and t_2, it does so along the path in configuration space for which the action is an extremum (normally a minimum). The minimum is the solution to the classical equation of motion, which is called the Euler-Lagrange equation. In particle physics this is known as the classical solution, which is motivated by the belief that a semiclassical approach may shed some light on the underlying quantum world. In quantum physics it often happens that the ground states are degenerate, that is there is more than one vacuum state. This problem may be cured by allowing quantum tunneling between states. The prescription on the tunneling is what is called an instanton. In the financial context this concept can be used to find the most probable path that makes the greatest contribution in the path integral, this is useful because in the case of complicated models the integral may be otherwise very difficult to perform. Moreover the structure of the process (usually modeling the option price or the log return) would not be known until the problem is actually solved, however with the instanton method it is possible to obtain a solution for the equation of motion, which describes the entire system, and at the same time shed some light on the structure of the process in question.

Mathematically the principle of least the action condition can be written as

$$\delta A = 0, \tag{51}$$

which leads to the Euler-Lagrange equation

$$\left[\frac{d}{dt}\left(\frac{\partial}{\partial\dot{\Omega}_i}\right)-\frac{\partial}{\partial\Omega_i}\right]\mathcal{L}(\Omega_i,\dot{\Omega}_i)=0. \tag{52}$$

Our Lagrangian has the form

$$\mathcal{L}(\Omega_i,\dot{\Omega}_i)=\frac{1}{2P[\Omega_i]^{1-q}}\dot{\Omega}^2 \tag{53}$$

where the functional $P[\Omega_i]^{1-q}$ is defined in Eq. (6). Hence the Lagrangian at a timeslice t_i may be written as

$$\mathcal{L}(\Omega_i,\dot{\Omega}_i)=\frac{Z^{(1-q)}(t_i)}{2\left[1-\beta(t_i)(1-q)\Omega_i^2\right]}\dot{\Omega}_i^2. \tag{54}$$

We now outline a general approach in evaluating the path integral in Eq. (50) using the instanton solution: first we write down the Lagrangian functional; using this functional, the Euler–Lagrange equation is then evaluated using Eq. (52) to obtain the equation of motion for the system. One then has to find the solution of the differential equation. This solution is then inserted into the path integral for evaluation; the option price using Eq. (18), with a given payoff function, in this case Eq. (43), is then calculated.

4.1. Keeping $Z^{(1-q)}(t_i)$ and $\beta(t_i)$ constant in time

Taking the derivative with respect to both Ω_i and $\dot{\Omega}_i$ and supposing that $Z^{(1-q)}(t_i)$ and $\beta(t_i)$ are constant in time, namely we define $Z^{(1-q)}(t_i) = Z^{(1-q)}$ and $\beta(t_i) = \beta$ respectively, leads to the following Euler-Lagrangian equation

$$\left[\frac{d}{dt}\left(\frac{\partial}{\partial\dot{\Omega}_i}\right) - \frac{\partial}{\partial\Omega_i}\right]\mathcal{L}(\Omega_i,\dot{\Omega}_i) = Z^{(1-q)}\left[\frac{\ddot{\Omega}_i\left[1-\beta(1-q)\Omega_i^2\right] + \dot{\Omega}_i^2\beta(1-q)\Omega_i}{\left[1-\beta(1-q)\Omega_i^2\right]^2}\right] = 0. \tag{55}$$

Now since $\left[1-\beta(1-q)\Omega_i^2\right] \neq 0$ similarly for $Z^{(1-q)} \neq 0$, we must have

$$\ddot{\Omega}_i\left[1-\beta(1-q)\Omega_i^2\right] + \dot{\Omega}_i^2\beta(1-q)\Omega_i = 0. \tag{56}$$

This equation is only true for $\beta(t_i)$ and $Z(t_i)$ constant in time, that is $\beta(t_i) \equiv \beta$ and $Z(t_i) = Z$.

In this case we may integrate and find that

$$\sinh^{-1}\left(\Omega_i\sqrt{\beta(1-q)}\right) = C_1 t_i - \Omega_i\sqrt{1-\beta(1-q)\Omega_i^2}, \tag{57}$$

where we have to solve for Ω_i.

4.2. The general case

We now return to the case when $\beta(t_i)$ and $Z(t_i)$ are not left constant but instead are allowed to vary with time, from Eqs. (7,8) and Eq. (10), we may take the time derivative of $\beta(t_i)$ and $Z(t_i)$ with $t' = 0$. In this case for $\beta'(t_i)$ we obtain the following expression,

$$\beta'(t_i) = \frac{d}{dt_i}\beta(t_i) = \pi^{\frac{1-q}{3-q}}\left[(2-q)(3-q)\,t_i\right]^{-\frac{2}{3-q}}\left(\frac{\Gamma\left[\frac{1}{q-1}-\frac{1}{2}\right]^2}{(q-1)\,\Gamma\left[\frac{1}{q-1}\right]^2}\right)^{\frac{1-q}{3-q}} = -\frac{2}{(3-q)\,t_i}\beta(t_i). \tag{58}$$

Similarly for the function $Z'(t_i)$

$$Z'(t_i) = \frac{d}{dt_i}Z(t_i) = \pi^{\frac{1}{3-q}}\left(\frac{(2-q)(3-q)\,t_i\,\Gamma\left[\frac{1}{q-1}-\frac{1}{2}\right]^2}{(q-1)\,\Gamma\left[\frac{1}{q-1}\right]^2}\right)^{\frac{1}{3-q}} = \frac{1}{(3-q)\,t_i}Z(t_i). \tag{59}$$

Now evaluating the Euler–Lagrange equation, we find that

$$\frac{\partial}{\partial\dot{\Omega}_i}\mathcal{L}(\Omega_i,\dot{\Omega}_i) = \frac{Z(t_i)^{1-q}\,\dot{\Omega}_i}{1-(1-q)\,\beta(t_i)\,{\Omega_i}^2} \tag{60}$$

$$\frac{\partial}{\partial\Omega_i}\mathcal{L}(\Omega_i,\dot{\Omega}_i) = \frac{(1-q)\,Z(t_i)^{1-q}\,\beta(t_i)\,\Omega_i\,\dot{\Omega}_i^2}{\left[1-(1-q)\,\beta(t_i)\,\Omega_i^2\right]^2}, \tag{61}$$

and taking the time derivative of Eq. (60),

$$\begin{aligned}\frac{d}{dt}\left(\frac{\partial}{\partial\dot{\Omega}_i}\right)\mathcal{L}(\Omega_i,\dot{\Omega}_i) &= \frac{Z(t_i)^{-q}}{\left[1-(1-q)\,\beta(t_i)\,\Omega_i^2\right]^2}\\ &\times \Big((1-q)\,\dot{\Omega}_i\,\left(\left[1-(1-q)\,\beta(t_i)\,\Omega_i^2\right]\,Z'(t_i)\right.\\ &+ \left.Z(t_i)\,\Omega_i\,\left(\Omega_i\,\beta'(t_i)+2\,\beta(t_i)\,\dot{\Omega}_i\right)\right)\\ &+ Z(t_i)\,\left[1-(1-q)\,\beta(t_i)\,\Omega_i^2\right]\,\ddot{\Omega}_i\Big). \end{aligned} \tag{62}$$

In this case the definition for the time derivative of $\dot{\Omega}(t_i)$ is equivalent to $\dot{\Omega}_i$, i.e. $\dot{\Omega}(t_i)\equiv\dot{\Omega}_i$, similarly for $\Omega(t_i)$ and $\ddot{\Omega}(t_i)$.

Combining terms in the previous equation leads to the following Euler–Lagrange equation,

$$\begin{aligned} 0 &= \left[\frac{d}{dt}\left(\frac{\partial}{\partial\dot{\Omega}_i}\right)-\frac{\partial}{\partial\Omega_i}\right]\mathcal{L}(\Omega_i,\dot{\Omega}_i)\\ &= \frac{Z(t_i)^{-q}}{\left[1-(1-q)\,\beta(t_i)\,\Omega_i^2\right]^2}\\ &\times \Big((1-q)\,\dot{\Omega}_i\,\left[\left[1-(1-q)\,\beta(t_i)\,\Omega_i^2\right]\,Z'(t_i)+Z(t_i)\,\Omega_i\,\left(\Omega_i\,\beta'(t_i)+\beta(t_i)\,\dot{\Omega}_i\right)\right]\\ &+ Z(t_i)\,\left[1-(1-q)\,\beta(t_i)\,\Omega_i^2\right]\,\ddot{\Omega}_i\Big). \end{aligned} \tag{63}$$

Now inserting Eqs. (58) and (59) into Eq. (63) we find that the Euler–Lagrange equation becomes

$$\begin{aligned} 0 &= \left[\frac{d}{dt}\left(\frac{\partial}{\partial\dot{\Omega}_i}\right)-\frac{\partial}{\partial\Omega_i}\right]\mathcal{L}(\Omega_i,\dot{\Omega}_i)\\ &= \frac{Z(t_i)^{1-q}}{\left[1-(1-q)\,\beta(t_i)\,\Omega_i^2\right]^2}\\ &\times \left[(1-q)\,\dot{\Omega}_i\,\left(\frac{\left[1-(1-q)\,\beta(t_i)\,\Omega_i^2\right]}{(3-q)\,t_i}+\Omega_i\,\left(-\frac{2\,\beta(t_i)\,\Omega_i}{(3-q)\,t_i}+\beta(t_i)\,\dot{\Omega}_i\right)\right)+\left[1-(1-q)\,\beta(t_i)\,\Omega_i^2\right]\,\ddot{\Omega}_i\right], \end{aligned} \tag{64}$$

dividing both sides of the equation by the factor sitting on the RHS we get

$$1+t_i\frac{(3-q)}{(1-q)}\frac{\ddot{\Omega}_i}{\dot{\Omega}_i}=\frac{\beta(t_i)\,\Omega_i\left[(3-q)t_i\,\dot{\Omega}_i-2\Omega_i\right]}{\left[1-(1-q)\,\beta(t_i)\,\Omega_i^2\right]}, \tag{65}$$

which is mathematically equivalent to

$$\begin{aligned}\dot{\Omega}_i\,\left[(1-q)-(3-q)\,(1-q)\,\beta(t_i)\,\Omega_i\,\left(\Omega_i-t_i\,\dot{\Omega}_i\right)\right]+\\ (3-q)\,t_i\,\left[1-(1-q)\,\beta(t_i)\,\Omega_i^2\right]\,\ddot{\Omega}_i=0.\end{aligned} \tag{66}$$

Eq. (65) is a non–trivial non–linear differential equation. Using Mathematica one obtains a following solution for Ω_i. Then by isolating irrelevant functions of q, to simplify the preceding equation, as follows

$$\gamma(q) = \pi^{\frac{q}{q-3}}\,(q-3)^{1+\frac{2}{q-3}}\,(q-2)^{\frac{2}{q-3}}\,(q-1)^{1+\frac{1}{q-3}}\,\Gamma\left[\frac{1}{q-1}-\frac{1}{2}\right]^{\frac{2\,q}{q-3}}\,\Gamma\left[\frac{1}{q-1}\right]^{\frac{2}{q-3}} \tag{67}$$

$$h(q) = \pi^{\frac{1}{q-3}}\,(q-3)\,(q-1)^{\frac{q}{q-3}}\,\Gamma\left[\frac{1}{q-1}-\frac{1}{2}\right]^{\frac{2}{q-3}}\,\Gamma\left[\frac{1}{q-1}\right]^{\frac{2\,q}{q-3}}, \tag{68}$$

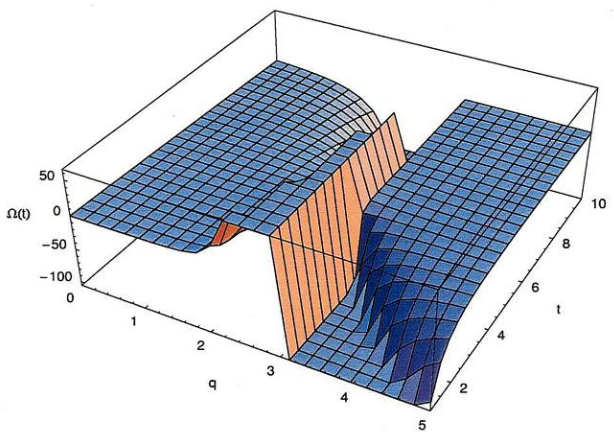

Figure 4. The graph of $\Omega(t)$ when $C_1 = C_2 = h(q) = 1$ and $\gamma(q) = 1$. The discontinuities become evident at $q = 3$.

we may rewrite the solution of the differential equation, Eq. (65), as

$$\Omega_i \to \frac{1}{8\,\eta(q)}\left(e^{-\frac{C_2\,\eta(q)}{q-3}}\,t_i^{-\frac{1+\eta(q)}{q-3}}\left(t_i^{\frac{2\,\eta(q)}{q-3}} - 16\,e^{2\left(C_1+\frac{C_2\,\eta(q)}{q-3}\right)}h(q)\right)\right) \tag{69}$$

$$\Omega_i \to \frac{1}{8\,\eta(q)}\left(e^{-\frac{C_2\,\eta(q)}{q-3}}\,t_i^{-\frac{1+\eta(q)}{q-3}}\left(e^{\frac{2\,C_2\,\eta(q)}{q-3}} - 16\,e^{2\,C_1}h(q)\,t_i^{\frac{2\,\eta(q)}{q-3}}\right)\right), \tag{70}$$

where the function $\eta(q)$ is given by $\eta(q) = \sqrt{1 + e^{2\,C_1}\gamma(q)}$.

Eqs. (69) and (70) are two equivalent solutions. We can therefore use both equations such that to extract the constant of integration one sets $\Omega(t_0) \equiv \Omega_0$ in Eq. (69) and $\Omega(t_0) \equiv \Omega_1$ in Eq. (70). We find that

$$C_1 = \frac{1}{2}\ln\left[\frac{16\,\Omega_1\,h(q)}{\Omega_0}\right], \tag{71}$$

$$C_2 = -\frac{1}{2}\ln(\Omega_1)\,\frac{(q-3)\sqrt{\Omega_0}}{\sqrt{\Omega_0 - \gamma(q)\Omega_1\,16\,h(q)}}. \tag{72}$$

In Fig. 4 we show graphically the structure of the solution by setting the constants to fixed values. In Fig. 4 we fix the $C_1 = C_2 = \gamma(q) = h(q) = 1$. If we set the constants to $C_1 = C_2 = h(q) = 1$ and $\gamma(q) = 10$ we would observe that as we increase the value of the $\gamma(q)$ by a factor of 10 the overall shape the graph remains almost identical, however, the value $\Omega(t)$ would scale up by a given factor, and the values of $\Omega(t)$ for $3 \leq q \leq 5$ are pushed further back in time. In the other region, the one for $0 \leq q \leq 3$ we would notice that the non–zero values for $\Omega(t)$ are shifted closer to the origin on the q axis. This is consistent with the fat-tail effect.

One thing that these two pictures have in common is the discontinuity around $q = 3$. Now looking at Eq. (67) through Eq. (72) we see that for $q \leq 3$, $\gamma(q)$ becomes complex. This is however not consistent with the initial value of $q = 1.43$ that was determined from empirical fits by Borland[5,6] on S&P 500 daily returns and NASDAQ stocks (1 minute interval). This represents a problem with the method, because if the q value extracted from the empirical data cannot be used without applying some sort of renormalization, it would mean that the information extracted from the empirical fit cannot be carried into the path integral approach. This issue must be explored further to address the problem to find a way around this problem and avoid complex integration in the path integral, Eq. (50), and see if this is specific to only one data set or not. One

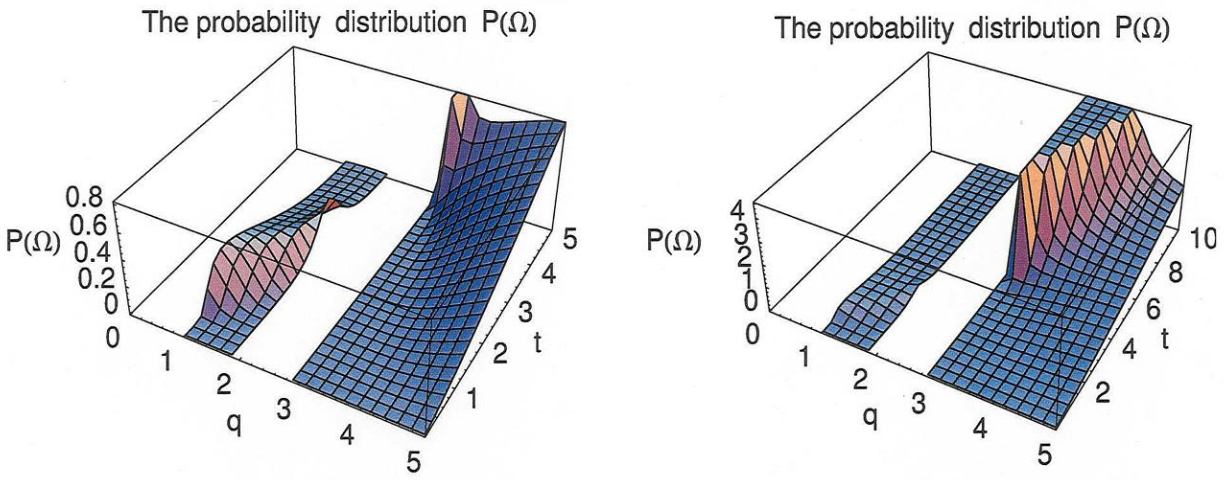

Figure 5. The graph of $P(\Omega(t))$ when $C_1 = C_2 = h(q) = 1$ and $\gamma(q) = 1$. The discontinuities become evident. The probability distribution function will be integrable in the region of $q \in [1,2]$ and $q \in [3,5]$ for small t. The left shows $P(\Omega)$ for $q \in [0,5]$ and $t \in [0.01,5]$, while the figure on the right shows the same graph but on a different t range, i.e. $t \in [0.01,10]$.

of the possibilities to avoid complex integration is to perform what is called a Wick rotation in physics. A Wick rotation consists of mapping the time onto the imaginary plane, this way a complex time variable would become real value variable.

Using the solution of Eq. (69), we can also graph the probability distribution function, in Eq. (6). In Fig. 5 and Fig. 6 we show the graph of the probability distribution $P(\Omega)$ for different t values and different plot ranges. In Fig. 5 (left graph) we show the probability distribution function, $P(\Omega)$, for $q \in [0,5]$ and $t \in [0,5]$, on this graph we can see where the function becomes complex valued and where it would be possible to integrate when this distribution is inserted into the the Lagrangian functional. From this graph we clearly see that in the range of $3 \leq q \leq 5$ the distribution is well behaved and that there are no discontinuities, moreover we can see that at around $t \geq 3$ the function is starting to sharply increase to a large value. Extending into the t direction to $t \leq 10$, shows that indeed there is a region where the distribution becomes singular, see Fig. 5 (right graph). If we now change the plotting range on both the t and the $P(\Omega)$ axis to see first how far the peak stretches and if there are other values of t for which we have a singularity, as it is done in Fig. 6, we remark that first there does not appear to be any other singularity points and that the distribution remains smooth elsewhere. Furthermore we observe that the singularity is finite.

We can also examine the distribution in the region of $q \in [1,2]$, the region where the value of $q = 1.43$ has been extracted from empirical fits; see Borland[5,6] for more details. This is shown in Fig. 7. where can see that the distribution is well behaved, without singularities or discontinuities thus permitting integration of $\Omega(t)$ with respect to t.

One of the main concerns with this solution is that now the range for the parameter q has been shifted from its previous value of 1.43. We see that the solution becomes complex for $q \leq 3$, because of the function $\gamma(q)$ not been well defined. This is because in Eq. (67) some of the terms are negative raised to a power, which is not defined in the real plane, that is the term $(q-3)^{1+\frac{2}{q-3}}\,(q-2)^{\frac{2}{q-3}} \notin \mathcal{R}$ for $q < 3$, while the term involving the Γ functions $\Gamma\left[\frac{1}{q-1} - \frac{1}{2}\right]^{\frac{2q}{q-3}} \Gamma\left[\frac{1}{q-1}\right]^{\frac{2}{q-3}}$ is defined in some of the regions for that q. On the other hand the

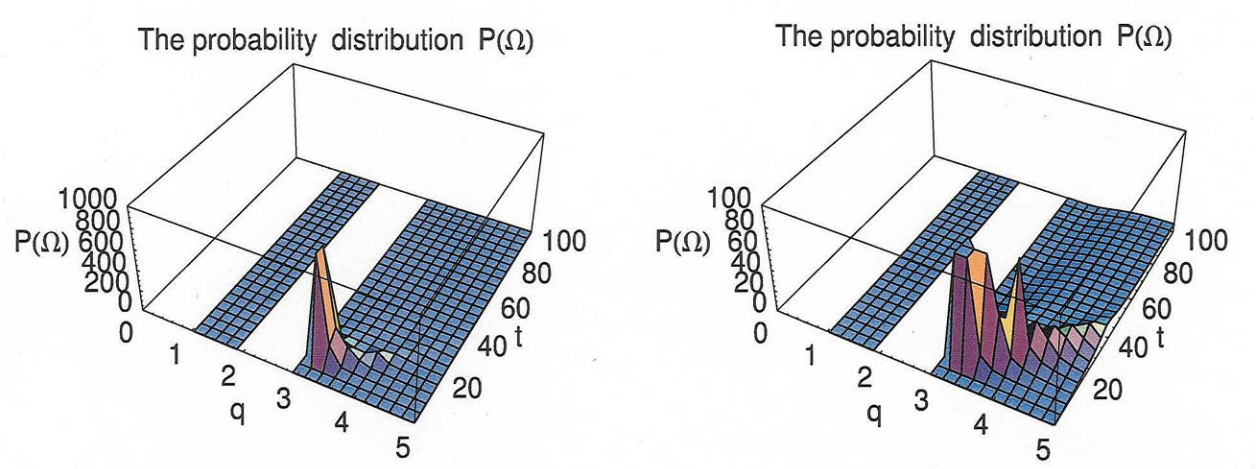

Figure 6. Same graph as in Fig. 5 for $P(\Omega(t))$ when $C_1 = C_2 = h(q) = 1$ and $\gamma(q) = 1$. Here the discontinuities become more evident. This shows the structure of the peak, which is finite. The probability distribution function will be integrable in the region of $q \in [1,2]$ and $q \in [3,5]$ for small t. The left shows $P(\Omega) \in [0,1000]$ for $q \in [0,5]$ and $t \in [0.01,100]$, while the figure on the right also shows $P(\Omega(t))$, but on a different range, i.e. $P(\Omega(t)) \in [0.01,100]$.

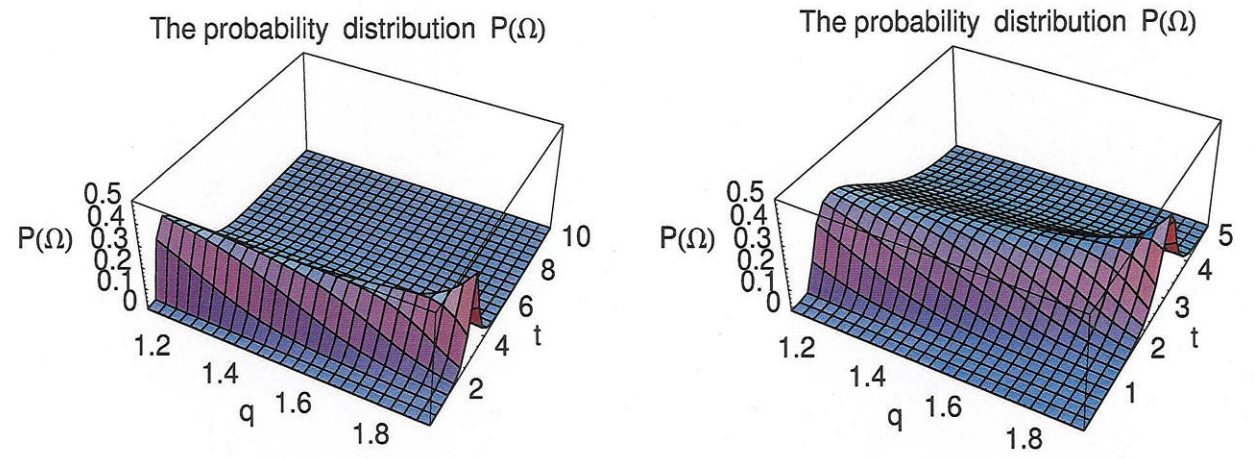

Figure 7. The graph of $\Omega(t)$ when $C_1 = C_2 = h(q) = 1$ and $\gamma(q) = 1$. Here q is taken in the range of $1.1 \leq q \leq 1.8$ in both figures. On the right graph the range for t is $0.01 \leq t \leq 5$ while on the left one the range is $0.01 \leq t \leq 10$.

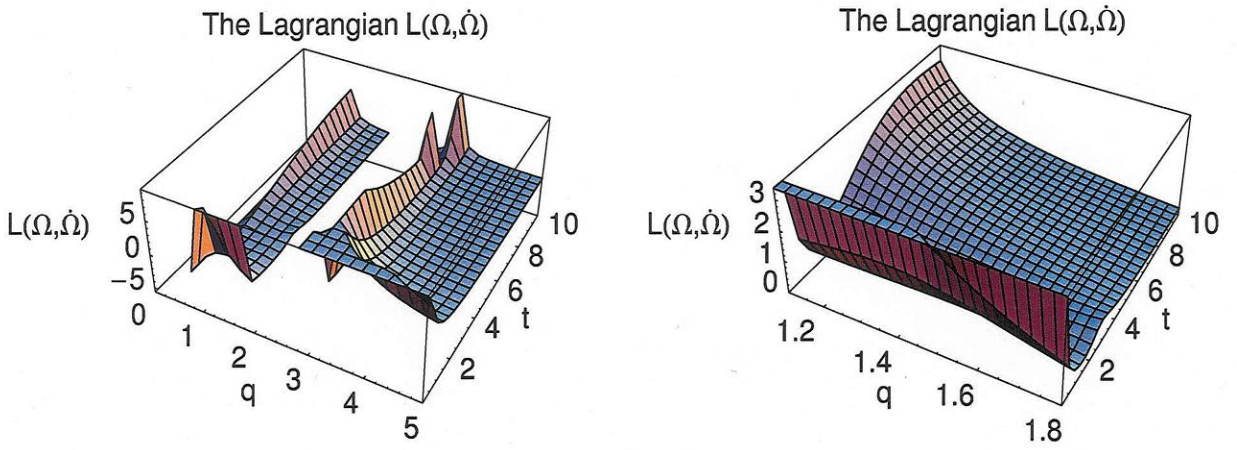

Figure 8. The graph of the Lagrangian functional Eq. (54) for a given $\Omega(t)$, Eq. (69), when $C_1 = C_2 = h(q) = 1$ and $\gamma(q) = 1$. Here t is taken in the range of $0.01 \leq t \leq 10$ in both figures. On the right graph the range for t is $1.1 \leq q \leq 1.8$ while on the left one the range is $0 \leq q \leq 5$.

first term just mentioned is perfectly defined for $q > 3$, while the term involving the Γ functions is not. As a result, combining the two terms together makes an undefined function, i.e. Eq. (67), for all q. This represents a problem as the integration of complex functions is no always well defined, but may be overcome by taking only the absolute values of the terms $q-3$ and $q-2$. In this case, in the region of $q \in [0,2]$, $\gamma(q)$ is well defined.

We can now examine the Lagrangian functional for the above case, as we did for the distribution $P(\Omega)$, which is for the case when $C_1 = C_2 = h(q) = 1$ and $\gamma(q) = 1$. This is shown in Fig. (8). Similarly, we can see from the left graph in Fig. 8 where the discontinuities are. In this case too, when we plot $L(\Omega, \dot{\Omega})$ in the region $q \in [1.1, 1.8]$, we have a well behaved functional that should be integrable without too many difficulties. See Fig. 8 (right graph).

To conclude this section, one can say that it is possible to perform the path integrations, provided we limit the range of the q value. This value must be extracted from real data and can only be within a small range, in this case it appears to be between 1 and 2, that is for $q \in [1,2]$.

4.2.1. The solution when $(q-3)^{1+\frac{2}{q-3}}\,(q-2)^{\frac{2}{q-3}} \longrightarrow (|q-3|)^{1+\frac{2}{q-3}}\,(|q-2|)^{\frac{2}{q-3}}$.

As just discussed in Section 4.2, the function $\gamma(q)$, Eq. (67), is not well defined for most values of q leading to a complex value solution and hence a complex path integral.

The problem may be addressed by setting $(q-3)^{1+\frac{2}{q-3}}\,(q-2)^{\frac{2}{q-3}} \longrightarrow (|q-3|)^{1+\frac{2}{q-3}}\,(|q-2|)^{\frac{2}{q-3}}$ in Eq. (67). The function $\gamma(q)$ then becomes

$$\begin{aligned}\gamma(q) &= \pi^{\frac{q}{q-3}}\,(q-3)^{1+\frac{2}{q-3}}\,(q-2)^{\frac{2}{q-3}}\,(q-1)^{1+\frac{1}{q-3}}\,\Gamma\left[\frac{1}{q-1}-\frac{1}{2}\right]^{\frac{2q}{q-3}}\,\Gamma\left[\frac{1}{q-1}\right]^{\frac{2}{q-3}} \\ &\longrightarrow \pi^{\frac{q}{q-3}}\,(|q-3|)^{1+\frac{2}{q-3}}\,(|q-2|)^{\frac{2}{q-3}}\,(q-1)^{1+\frac{1}{q-3}}\,\Gamma\left[\frac{1}{q-1}-\frac{1}{2}\right]^{\frac{2q}{q-3}}\,\Gamma\left[\frac{1}{q-1}\right]^{\frac{2}{q-3}}. \qquad (73)\end{aligned}$$

This has the effect of only considering the absolute value of $q-3$ and $q-2$ for all q. In that case it is then

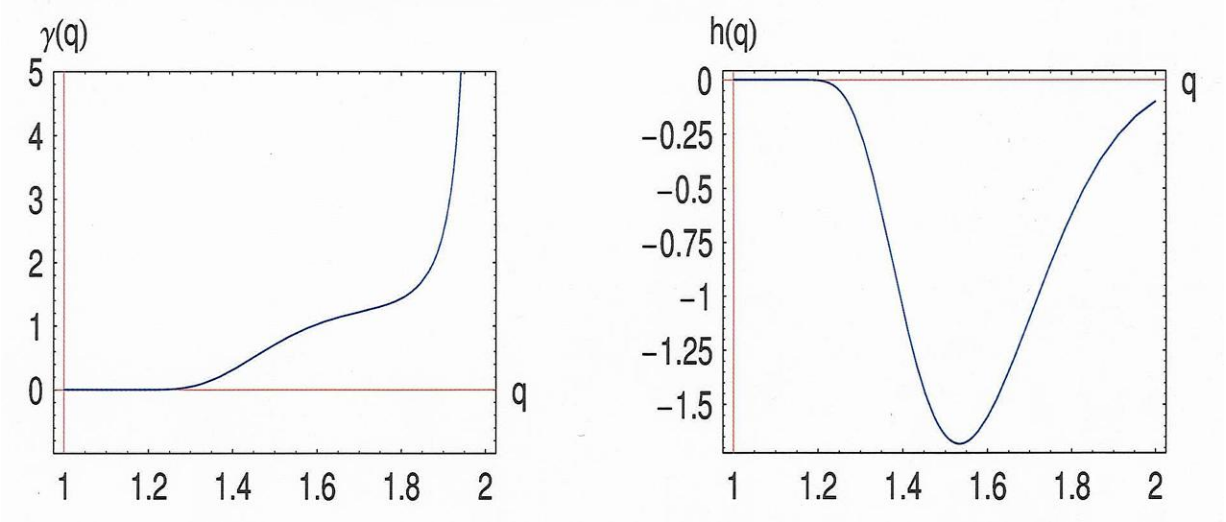

Figure 9. The graph of the functions $\gamma(q)$, Eq. (67), (left figure) and $h(q)$, Eq. (68), (right figure) as a function of q for $q \in [1,2]$ when the terms $(q-3)^{1+\frac{2}{q-3}}\,(q-2)^{\frac{2}{q-3}}$ in Eq (67) are set to $(|q-3|)^{1+\frac{2}{q-3}}\,(|q-2|)^{\frac{2}{q-3}}$.

possible to obtain a graph for $\gamma(q)$ and $h(q)$, that is Eq. (67) and Eq. (68) respectively, as a function of q on a small interval.

In Fig. 9 we show the graph of $\gamma(q)$ (left graph) and $h(q)$ (right graph) as a function of q. In these graphs we can see the shape of the curve, and we can also see that $\gamma(q) = 0$ for $q \leq 1.25$. For $q \in [1.25, 1.8]$ the function is stable, while for $q \geq 1.8$ it strongly diverges to a large value. Now looking at the right graph in Fig. 9, that is the graph for $h(q)$, on the interval of $q \in [1,2]$ we see a well behaved function. If we look outside this interval $h(q)$ becomes a highly oscillating function for $q < 1$, while remaining finite and non–divergent, at $q = 2$ and $q = 3$ it is zero.

Combining the Eqs. (68) and Eq. (73) into Eq. (71) and Eq. (72), setting $\Omega_0 = \Omega_1 = 1$ in C_1 and $\Omega_0 = 1$, $\Omega_1 = 2$ in C_2, it is possible to graph the coefficients C_1 and C_2, defined in Eq. (71) and Eq. (72) respectively, as seen Fig. 10. On the left graph of Fig. 10 we show the graph of the coefficient C_1 on a large q interval, i.e. $q \in [-5,5]$. From this graph it is very easy to see how the function behaves. We can also see regions where it is possible to use these coefficients. Especially in the region of $q \in [1,2]$ where we see a perfectly smooth function. As for C_2, which is graphed on the right hand side of Fig. 10, there too we find a smooth function for $q \in [1,2]$. Although not shown on the figure, for $q \leq 1$ we observed a highly oscillating function with non divergent sharp peaks and for $q \geq 3$, $C_2 = 0$.

We can proceed in graphing $\Omega(t)$ with the above functions as input. In Fig. 11 the graph of $\Omega(t)$ is shown on two different q intervals, that is $q \in [1.1, 1.99]$ on the right and $q \in [0,5]$ on the left. On both graphs $\Omega(t)$ is plotted over $t \in [0.01, 10]$. On the left graph we notice that $\Omega(t)$ take a very large value for $q \to 3$. This is due to the C_1 and $\gamma(q)$ contributions in the terms involving these two in Eq. (69) and Eq. (70). Looking at the right graph in Fig. 11 we see a smooth and non divergent surface. In Fig. 12 we show the plot of the probability distribution function $P(\Omega)$ for the same q interval but on two different t intervals. In a similar way we obtain a graph for the Lagrangian density, $L(\Omega, \dot{\Omega})$. This is shown in Fig. 13.

To summarize, it is possible to avoid the problem of complex integration in the path integral, Eq. (50), because of $\gamma(q)$ being not well defined for all q, and certainly not for the q value extracted from empirical data in Borland.[5,6] However by setting $(q-3)^{1+\frac{2}{q-3}}\,(q-2)^{\frac{2}{q-3}} \longrightarrow (|q-3|)^{1+\frac{2}{q-3}}\,(|q-2|)^{\frac{2}{q-3}}$ in Eq. (67)

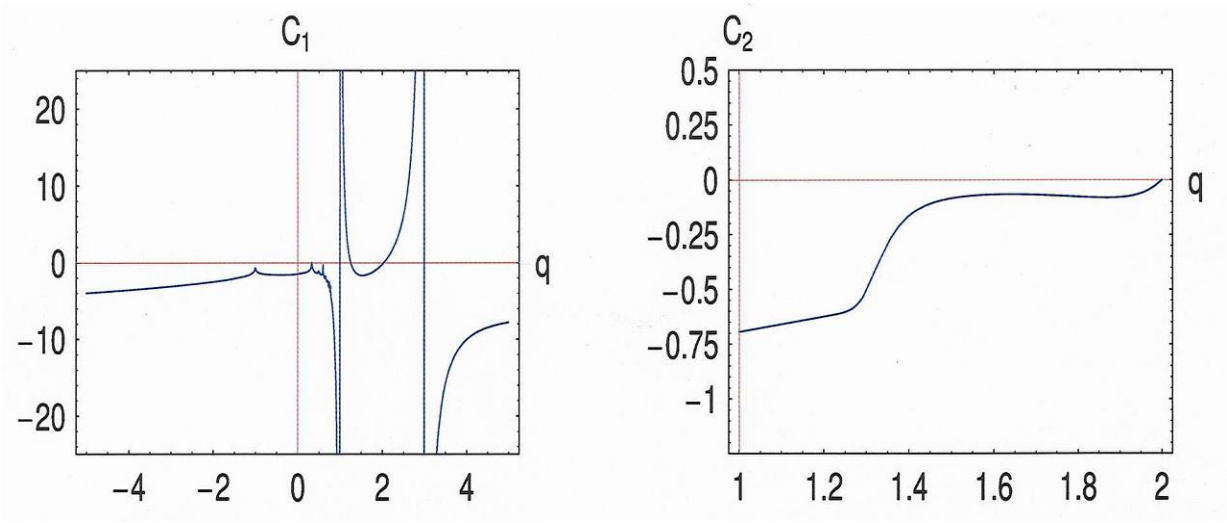

Figure 10. The graph of the coefficients C_1, Eq. (71) (left graph), and C_2, Eq. (72) (right graph) as a functions q with the functions $\gamma(q)$, Eq. (67) and $h(q)$, Eq. (68) as a function of q for $q \in [1,2]$ when the terms $(q-3)^{1+\frac{2}{q-3}}\,(q-2)^{\frac{2}{q-3}}$ in Eq (67) are set to $(|q-3|)^{1+\frac{2}{q-3}}\,(|q-2|)^{\frac{2}{q-3}}$.

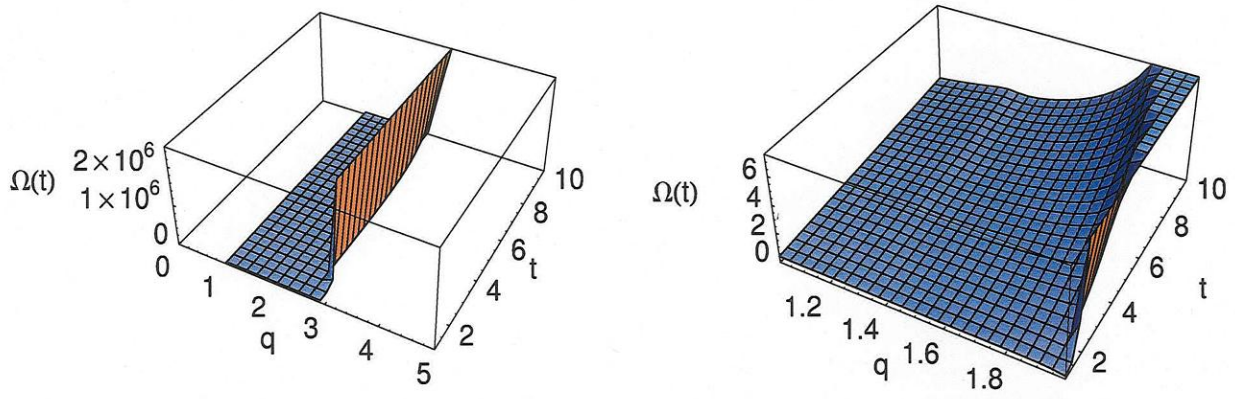

Figure 11. The graph of the solution $\Omega(t)$ for two different q intervals (left figure $q \in [0,5]$ and for $q \in [1.1, 1.99]$ on the right figure). Here the coefficients C_1, Eq. (71), and C_2, Eq. (72), are functions of q with the above functions $\gamma(q)$, Eq. (67), and $h(q)$, Eq. (68), as a function of q for $q \in [1,2]$ when the terms $(q-3)^{1+\frac{2}{q-3}}\,(q-2)^{\frac{2}{q-3}}$ in Eq (67) are set to $(|q-3|)^{1+\frac{2}{q-3}}\,(|q-2|)^{\frac{2}{q-3}}$.

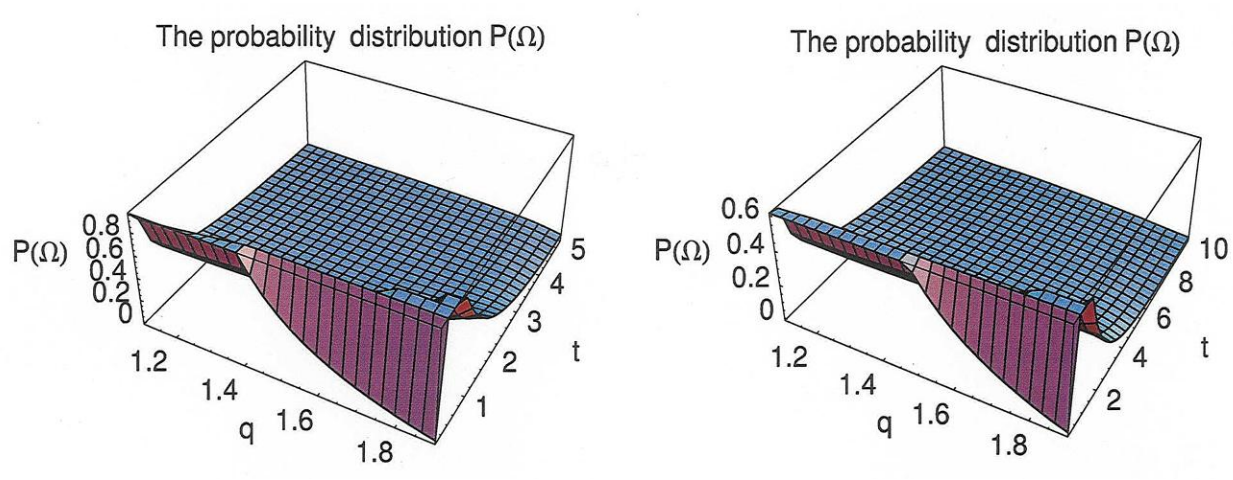

Figure 12. The graph of the probability distribution function $P(\Omega)$ using the solution $\Omega(t)$ for two different t intervals (left figure $t \in [0, 5]$ and $t \in [0, 10]$ on the right figure, both figures are plotted over $q \in [1.1, 1.99]$). Here the coefficients C_1, Eq. (71), and C_2, Eq. (72), are functions of q with the above functions $\gamma(q)$, Eq. (67), and $h(q)$, Eq. (68), as a function of q for $q \in [1, 2]$ when the terms $(q-3)^{1+\frac{2}{q-3}}\,(q-2)^{\frac{2}{q-3}}$ in Eq (67) are set to $(|q-3|)^{1+\frac{2}{q-3}}\,(|q-2|)^{\frac{2}{q-3}}$.

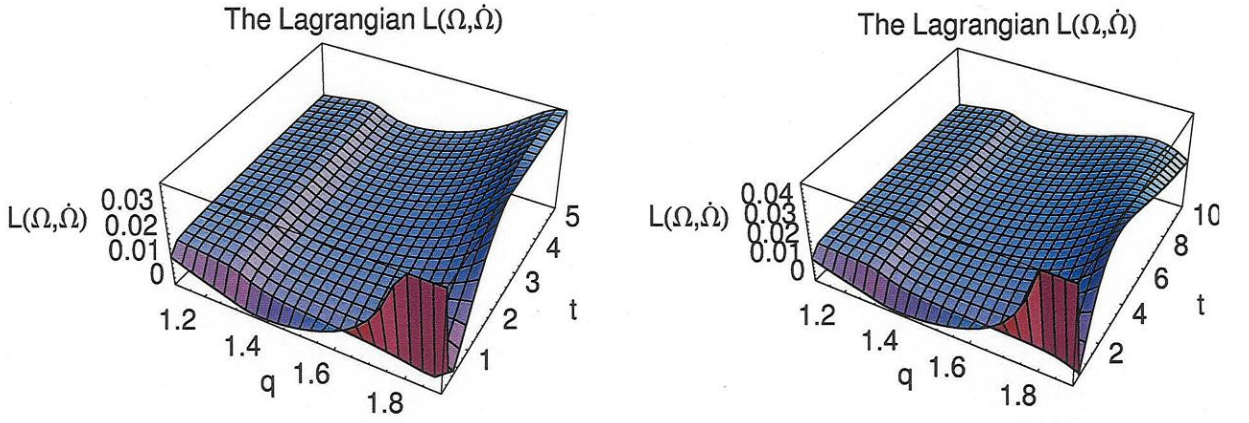

Figure 13. The graph of the Lagrangian density function $L(\Omega, \dot{\Omega})$ using the solution $\Omega(t)$ and the probability distribution function plotted in Fig. 12 for two different t intervals (left figure $t \in [0, 5]$ and $t \in [0, 10]$ on the right figure, both figures are plotted over $q \in [1.1, 1.99]$). Here the coefficients C_1, Eq. (71), and C_2, Eq. (72), are functions of q with the above functions $\gamma(q)$, Eq. (67), and $h(q)$, Eq. (68), as a function of q for $q \in [1, 2]$ when the terms $(q-3)^{1+\frac{2}{q-3}}\,(q-2)^{\frac{2}{q-3}}$ in Eq (67) are set to $(|q-3|)^{1+\frac{2}{q-3}}\,(|q-2|)^{\frac{2}{q-3}}$.

and $\sqrt{\Omega_0 - \gamma(q)\Omega_1 16\,h(q)} \longrightarrow \sqrt{|\Omega_0 - \gamma(q)\Omega_1 16\,h(q)|}$, in Eq. (72), it is possible to obtain smooth surfaces for the solution $\Omega(t)$ of the Euler–Lagrange, Eq. (65). Similarly for the probability distribution function, $P(\Omega)$, and consequently for the Lagrangian density $L(\Omega, \dot{\Omega})$ for a small q region, i.e. $q \in [1.1, 1.99]$. As a result it is possible to carry out the integrations of the path integral, Eq. (50).

5. CONCLUSION AND OPEN QUESTIONS

We have described and derived the path integral for a non–Gaussian option pricing model. We see that the path integral takes a relatively simple form, which is governed by the structure of the action taken into consideration. Since the path integral is a functional of Ω_i we see that functional derivatives appear in the path integral. We therefore proceeded in finding the path that contributes most to the action by finding the local minima of the action functional. This is commonly known as the instanton solution in physics.

The next step in our future work is to perform calculations using path integrals and compare the results from different stochastic models with real evolution of stock, option and bond prices. This work did not take into consideration the normalization of the propagator function in Eq. (50). This may be a necessary step in avoiding the problem of complex integration discussed in Sec. 4.2. This will be considered in future work.

6. ACKOWLEDGEMENT

We are very grateful to Lisa Borland and Jean-Philippe Bouchaud for instructive discussion. Funding from the Australian research council (ARC) is gratefully acknowledged.

REFERENCES

1. J.-P. Bouchaud, G. Iori, and D. Sornette, "Real world options: Smile and residual risk," *Risk* **93**, pp. 61–65, 1996.
2. J.-P. Bouchaud and M. Potters, *Theory of Financial Risks*, Cambridge University Press, Cambridge, 2000.
3. R. C. Merton, "Option pricing when underlying stock returns are discontinuous," *J. Fin. Econ.* **3**, pp. 125–144, 1976.
4. J. Hull, *Option, Futures, and other Derivatives*, 4th edn. Prentice Hall, Wiley, New Jersey, 2000.
5. L. Borland, "A theory of non-Gaussian option pricing," *Quantitative Finance* **2**, pp. 415–431, 2002.
6. L. Borland and J.-P. Bouchaud, "A non-Gaussian option pricing model with skew," `cond mat/0403022v2` , 2004.
7. L. Borland, "Microscopic dynamics of the nonlinear Fokker-Planck equation: A phenomenological model," *Phys. Rev. E* **57**, p. 6634, 1998.
8. C. Tsallis, "Possible generalization of Boltzmann-Gibbs statistics," *J. Stat. Phys.* **52**, p. 479, 1988.
9. E. Curado and C. Tsallis, "Generalized statistical mechanics: connection with thermodynamics," *J. Phys. A: Math. Gen.* **24**, p. L69, 1991.
10. V. Linetsky, "The path integral approach to financial modeling and option pricing," *Computational Economics* **11**, pp. 129–163, 1998.
11. F. Black and M. Scholes, "Equations of state calculations by fast computing machine," *J. Pol. Econ.* **81**, p. 637, 1973.
12. R. C. Merton, "Theory of rational option pricing," *Bell J. Econ. Management Sci.* **4**, pp. 141–183, 1973.
13. R. P. Feynman, "Space-time approach to non-relativistic quantum mechanics," *Rev. Mod. Phys.* **20**, p. 367, 1948.
14. C. Grosche and F. Steiner, "How to solve path integrals in quantum mechanics," *J. Math. Phys.* **36 (5)**, p. 2354, 1995.